Pharmaceutical Research, Vol. 8, No. 12, 1991

Research Article

The Influence of Peptide Structure on Transport Across Caco-2 Cells

Robert A. Conradi,[1] Allen R. Hilgers,[1] Norman F. H. Ho,[1] and Philip S. Burton[1,2]

Received June 14, 1990; accepted June 12, 1991

The relationship between structure and permeability of peptides across epithelial cells was studied. Using confluent monolayers of Caco-2 cells as a model of the intestinal epithelium, permeability coefficients were obtained from the steady-state flux of a series of neutral and zwitterionic peptides prepared from D-phenylalanine and glycine. Although these peptides ranged in lipophilicity (log octanol/water partition coefficient) from −2.2 to +2.8, no correlation was found between the observed flux and the apparent lipophilicity. However, a strong correlation was found for the flux of the neutral series and the total number of hydrogen bonds the peptide could potentially make with water. These results suggest that a major impediment to peptide passive absorption is the energy required to break water–peptide hydrogen bonds in order for the solute to enter the cell membrane. This energy appears not to be offset by the favorable introduction of lipophilic side chains in the amino acid residues.

KEY WORDS: peptide; transport; permeability; lipophilicity; hydrogen bonding; cell culture.

INTRODUCTION

The successful development of peptides and peptide-like hormones as orally bioavailable therapeutic agents remains a significant challenge to the pharmaceutical scientist. Such efforts will clearly be aided by a better understanding of the influence of peptide structure on transport across the intestinal mucosa. In an attempt to define such relationships, we have been examining the transport of model peptides across the intestinal epithelium. Preliminary reports from this laboratory with a series of oligomers prepared from phenylalanine and glycine suggested that both charge and chain length were more important than lipophilicity in predicting the flux of such peptides across rabbit intestine (1,2).

Several years ago, Stein showed that the transport of a series of solutes into a variety of plant and animal cells was highly correlated with the number of hydrogen bonds that the solute could make with water (3). He found that, as the number of potential solute–solvent hydrogen bonds increased, the permeability of the solute decreased. This was consistent with a requirement for the desolvation of the solute before transport across the cell membrane.

Since a general feature of peptides is the presence of numerous potential hydrogen-bonding sites in the polypeptide backbone, it seemed reasonable that a similar argument might explain the decreased transport of the phenylalanine oligomers with increasing chain length we had observed previously. In order to test this concept, the transport of the same series of peptides was examined across confluent monolayers of Caco-2 cells. These cells have been shown by several laboratories to represent a sensitive, reproducible *in vitro* model of the intestinal epithelium for the study of drug transport (4–6). Also, in order to increase the number of hydrogen-bonding solutes for this analysis, the transport of several additional small amides was determined.

MATERIALS AND METHODS

Materials. Glycine, ethylester hydrochloride, [glycine-1-^{14}C], specific activity 50 mCi/mmol, acetic anhydride, [1-^{14}C], 7 mCi/mmol, and mannitol, D-[1-^{14}C], 49 mCi/mmol, were obtained from New England Nuclear. Acetic anhydride, [1-^{14}C], 106 mCi/mmol, was purchased from Amersham. *N*-t-BOC[3]-D-Phenylalanine was from Sigma. All other reagents were from Aldrich and were of analytical grade. Chromatography solvents were from Burdick and Jackson. Caco-2 cells were obtained from ATCC at passage 13. All cell culture reagents were from GIBCO. Transwell inserts were from Costar.

General Synthetic Methods. Standard solution methodology as illustrated in Schemes I and II was used for the synthesis of the unlabeled peptides I–VI (Fig. 1). These were then purified and characterized. The radiolabeled analogues were then prepared under identical conditions and compared to the authentic standards.

Reverse-phase HPLC (RP-HPLC) was performed on a

[1] Drug Delivery Systems Research, The Upjohn Company, Kalamazoo, Michigan 49001.

[2] To whom correspondence should be addressed.

[3] Abbreviations used: HOSu, *N*-hydroxysuccinimide; DCC, dicyclohexylcarbodimide; TFA, trifluoroacetic acid; DMOA, *N,N*-dimethyloctylamine; BOC, tertiary butyloxycarbonyl; HBSS, Hank's balanced salt solution; TLC, thin-layer chromatography; RP-HPLC, reverse-phase high-performance liquid chromatography.

0724-8741/91/1200-1453$06.50/0

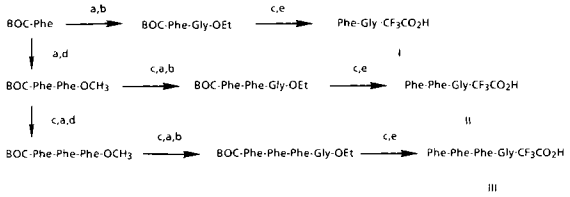

Scheme I. Preparation of peptides I–III. (a) HOSu, DCC, $CHCl_3$. (b) Gly-OEt, Et_3N, $CHCl_3$. (c) 1 *N* NaOH, THF. (d) Phe-OCH_3. (e) CF_3CO_2H, CH_2Cl_2.

system consisting of a Beckman Model 110A pump, Perkin-Elmer LC-55-B detector, and HP-3380A integrator. The column was a Brownlee RP-18, Spheri-5, 4.6 mm × 10 cm, with a 2-cm guard. Detection was typically at 205 nm. For the radiolabeled peptides detection was with a Flo-One HS detector from Radiomatic fitted with a 250-μl flow cell. The flow rate was maintained at 1 ml/min with a scintillant (Flo-Scint II) to column effluent ratio of 4:1. Preparative thin-layer chromatography (TLC) was performed on 20 × 20-cm silica gel G plates from Analtech.

D-*Phenylalanylglycine, [Glycine-1-^{14}C], Trifloroacetate (I).* To a solution of BOC-D-Phe (25 mg, 0.09 mmol) in 1 ml $CHCl_3$ were added HOSu (12 mg, 0.01 mmol) and DCC (21.5 mg, 0.1 mmol). After stirring for 20 min, the solution was filtered, and a mixture of glycine [1-^{14}C]ethyl ester hydrochloride (250 μCi, 0.005 mmol) and triethylamine (2 ml, 0.014 mmol) in 1 ml $CHCl_3$ was added to the filtrate. After stirring an additional 2 hr, the solution was washed with 5% (v/v) HCl, water, then dried over Na_2SO_4, and the product was concentrated under a N_2 stream. The resulting concentrate was applied to a prep silica gel plate and developed with isopropanol–$CHCl_3$ (5:95). The product was extracted from the gel with CH_3OH–$CHCl_3$ (20:80). After removal of solvent, the residue was dissolved in 0.5 ml THF, 0.1 ml 1 *N* NaOH added, and the resulting solution stirred overnight. This solution was again concentrated to a small volume under N_2, 0.05 ml 3 *N* HCl added, and the BOC-PheGly product extracted into $CHCl_3$. After removal of the solvent, the residue was redissolved in CF_3CO_2H–CH_2Cl_2 (50:50) and let stand for 30 min. Final removal of solvent and trituration with diethylether yielded 180 μCi of the desired product with a specific activity of 47 μCi/μmol. Mass spectrometry (nonradiolabeled peptide), $[M + H]^+$ at 222. RP-HPLC, 6.6-min retention time (15% CH_3CN, 0.02% CF_3CO_2H, 0.02% DMOA at 1 ml/min).

D-*Phenylalanyl-D-Phenylalanylglycine, [Glycine-1-^{14}C], Trifluoroacetate (II).* Preparation was similar to that of I, starting with Boc-D-Phe-D-Phe. The BOC-D-Phe-D-Phe-Gly ethyl ester was purified by preparatory TLC, eluting with methanol–chloroform (5:95). Yield of II was 88 μCi at a specific activity of 49 μCi/μmol. Mass spectrometry (nonradiolabeled peptide), $[M + H]^+$ at 370. RP-HPLC, 8.12-min retention time (8% CH_3CN, 0.02% CF_3CO_2H, 0.02% DMOA at 1 ml/min).

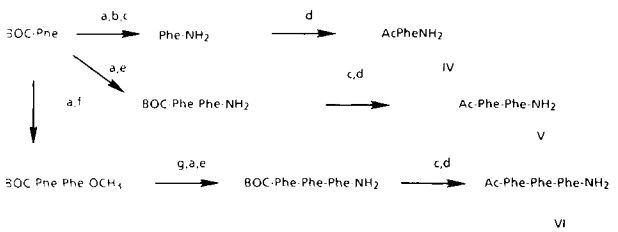

Scheme II. Preparation of peptides IV–VI. (a) HOSu, DCC, $CHCl_3$. (b) NH_3 (g). (c) CF_3CO_2H, CH_2Cl_2. (d) $(CH_3CO)_2O$, THF. (e) Phe-NH_2, $CHCl_3$. (f) Phe-OCH_3, $CHCl_3$. (g) 1 *N* NaOH, THF.

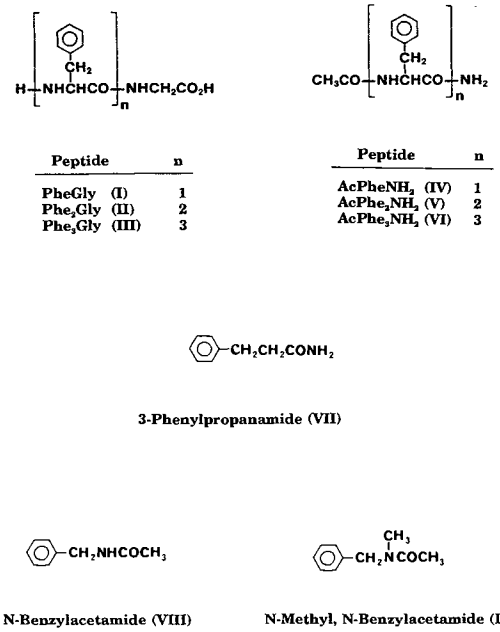

Fig. 1. Structures of the peptide solutes.

D-*Phenylalanyl-D-Phenylalanyl-D-Phenylalanylglycine, [Glycine-1-^{14}C], Trifluoroacetate (III).* Preparation was similar to that of I, starting with BOC-D-Phe-D-Phe-D-Phe. The Boc-D-Phe-D-Phe-Gly ethyl ester was purified by preparatory TLC, eluting with methanol–chloroform–ammonium hydroxide (5:95:0.01). Yield of III was 35 μCi with a specific activity of 49 μCi/μmol. Mass spectrometry (nonradiolabeled peptide), $[M + H]^+$ at 517. RP-HPLC, 2.61-min retention time (30% CH_3CN, 0.02% CF_3CO_2H, 0.02% DMOA at 1 ml/min).

Acetamido-D-Phenylalanylcarboxamide, [Acetyl-1-^{14}C] (IV). To a solution of D-Phe-NH_2 (6 mg, 0.04 mmol) in 1 ml $CHCl_3$ was added acetic anhydride [1-^{14}C] (500 μCi, 0.0047 mmol), in 0.25 ml toluene. After stirring overnight, the solvent was evaporated under N_2, and the residue chromatographed on preparatory TLC, eluting with methanol–chloroform (10:90). The product band was cut out and extracted with methanol–chloroform (50:50) to yield 155 μCi of the peptide with a specific activity of 106 μCi/μmol. Mass spectrometry (nonradiolabeled peptide), M^+ at 206. RP-HPLC, 9.0-min retention time (10% CH_3CN, 0.02% CF_3CO_2H, 0.02% DMOA at 1 ml/min).

Acetamido-D-Phenylalanyl-D-Phenylalanylcarboxamide, [Acetyl-1-^{14}C] (V). Preparation was as for IV, starting with D-Phe-D-Phe-NH_2. Purification on preparatory TLC with isopropanol–chloroform (10:90) yielded 15 μCi of product with a specific activity of 106 μCi/μmol. Mass spectrometry (nonradiolabeled peptide), M^+ at 353. RP-HPLC, 6.1-min retention time (30% CH_3CN, 0.02% CF_3CO_2H, 0.02% DMOA at 1 ml/min.

Acetamido-D-Phenylalanyl-D-Phenylalanyl-D-Phenylalanylcarboxamide, [Acetyl-1-^{14}C] (VI). Preparation was as for IV, starting with D-Phe-D-Phe-D-Phe-NH_2. Purification

on preparatory TLC, eluting with isopropanol–chloroform–ammonium hydroxide (10:90:0.01), yielded 36 μCi of the desired product with a specific activity of 106 μCi/μmol. Mass spectrometry (nonradioactive peptide), M^+ at 500. RP-HPLC, 6.2-min retention time (40% CH_3CN, 0.02% CF_3CO_2H, 0.02% DMOA at 1 ml/min).

3-Phenylpropanamide (VII). Hydrocinnamoyl chloride was treated with aqueous ammonia under standard conditions (7). The product was purified by crystallization from water. MP 148–150°C, lit. 149.2°C.

N-Benzylacetamide, [Acetyl-1-^{14}C] (VIII). To a solution of *N*-benzylamine (8 μl, 0.07 mmol) and triethylamine (10 μl, 0.07 mmol) in $CHCl_3$ was added acetic anhydride, [1-^{14}C] (250 μCi, 0.035 mmol). After stirring for 1 hr, the solution was washed with 5% HCl (v/v), 10% Na_2CO_3, dried, and filtered. After chromatography on TLC eluting with methanol–chloroform–ammonium hydroxide (5:95:0.1), 110 μCi of product was obtained with a specific activity of 7 μCi/μmol. The product was shown to be chromatographically identical to an authentic standard from CTC Organics.

N-Benzyl,N-methylacetamide (IX). This compound was prepared as described previously (8).

Solubility Determinations. The aqueous solubilities of the peptides were determined after equilibration in Krebs–Ringer buffer (25°C, pH 7.4). An excess of solid was shaken for 24, 48, and 72 hr. The supernatant was assayed by HPLC after filtration through a 0.22-μm Millipore filter which had been presaturated with the peptide of interest in order to inhibit nonspecific binding to the filter.

Partition Coefficient Determinations. Octanol/Krebs–Ringer partition coefficients were determined by shaking buffered aqueous solutions of the solute with buffer-saturated octanol overnight. After centrifugation to separate the phases, peptide concentrations were determined by either HPLC or liquid scintillation counting. The partition coefficients are reported as the log of the concentration in the octanol divided by the concentration in the aqueous phase.

Cell Culture. The preparation of confluent Caco-2 cell monolayers on Transwell polycarbonate filters has been described in detail previously (6). The cells used in this study were between passage number 26 and passage number 40.

Transport Studies. The transport experiments were performed with monolayers of between 14 and 21 days in culture as described previously (6). Briefly, the monolayers were washed three times with HBSS before the solute of interest (in HBSS) was added to the donor compartment. Donor concentrations were typically 2–10 μ*M* for the radiolabeled solutes and 0.2–0.3 m*M* for the unlabeled solutes.

After incubation at 37°C for a specific interval, the cup containing the monolayer and donor solution was transferred to a fresh receiver compartment. In order to maintain sink conditions in the receivers, transfer intervals were chosen such that approximately 5% or less of the solute moved from the donor to the receiver during the equilibration. At the end of the experiment, aliquots of the donor and receiver compartments were assayed for the appropriate substrate. Effective permeability coefficients (P_{eff}) were calculated from these results as before (6).

Finally, the first time a transport study was performed with a solute, aliquots of the donor and receiver were chromatographed to assure that the radioactivity measured was associated with the parent peptide, and not radioactive fragments which may have resulted from cell-mediated metabolism.

Cell Toxicity of Peptides IV and V. In order to establish that the fluxes observed for the most permeable peptides were not due to artifacts resulting from toxic effects of the peptides on the Caco-2 cell monolayers, two experiments were performed. In one series, [^{14}C]mannitol, as a cell-impermeable marker, was included in 0.3 and 1.28 m*M* solutions of unlabeled peptide V. The flux of mannitol was followed in this case. No increase in mannitol flux over 6 hr was seen with either of these solutions relative to non-peptide-containing buffer controls.

In a second experiment, monolayers were incubated in either the presence or the absence of 0.3 m*M* peptide IV. After 3 hr, the cells were removed from the filters by trypsinization and examined for viability by their ability to exclude trypan blue. No evidence of peptide induced cell toxicity was observed by this criterion.

Analytical Methods. Mass spectral analysis was performed by the Upjohn Physical and Analytical Chemistry Department. Radioactivity was quantitated by liquid scintillation counting with a Beckman LS 3801 scintillation counter. 3-Phenylpropanamide and *N*-Methyl,*N*-benzylacetamide were quantitated by RP-HPLC. An isocratic solvent system was employed for both compounds consisting of 25% acetonitrile containing 0.02% trifluoroacetic acid at a flow rate of 2 ml/min and detection at 205 nm. Under these conditions retention times were 2.0 min for 3-phenylpropanamide and 3.6 min for *N*-Methyl,*N*-benzylacetamide, respectively.

RESULTS

Physical Properties of the Peptides. The molecular weights, solubilities in Krebs–Ringer buffer, and octanol–buffer partition coefficients for peptides I to VI are summarized in Table I. Peptides I to III are zwitterions at physiological pH and, consistent with this structure, show little tendency to partition into the octanol phase. However, the increase in phenylalanyl groups through the series results in enhanced distribution because of the increase in hydrocarbon content in the amino acid side chain.

Peptide IV is formally a phenylalanylglycine dipeptide as is I except that the elements of glycine are used to block the amino and carboxyl groups. As can be seen from Table I, this modification results in a substantially more lipophilic peptide with a concomitant decrease in overall solubility.

Table I. Properties of the Zwitterionic and Neutral Phenylalanine Oligimers

Peptide	MW	Solubility[a]	log partition coefficient[b]
PheGly (I)	222	750,000	−2.16
Phe_2Gly (II)	369	340	−1.46
Phe_3Gly (III)	516	52	−0.66
$AcPheNH_2$ (IV)	206	71,570	0.05
$AcPhe_2NH_2$ (V)	353	70	1.19
$AcPhe_3NH_2$ (VI)	500	40	2.30

[a] μg/ml at pH 7.4.
[b] Octanol–Kreb's Ringer buffer (pH 7.2).

Further, similar to the zwitterionic series, addition of more phenylalanyl residues to give V and VI yielded peptides with increasing lipophilicity accompanied by a substantial decrease in water solubility. For this series, each phenylalanyl residue contributes approximately one log unit to the partition coefficient.

Flux of Peptides I–VI Across Caco-2 Cell Monolayers. The cumulative appearance of zwitterionic peptides I–III and the neutral series IV–VI in the receiver compartments is shown in Figs. 2 and 3. Similar to what was found with rabbit intestine, increasing the chain length in either series results in a marked decrease in flux. No metabolism was found for any of these peptides by chromatography of the donor and receiver compartments at the end of the experiment. Further, greater than 95% of the total radioactivity could be accounted for in the donor and receiver solutions, suggesting minimal peptide adsorption to the cell monolayer or Transwell system itself at the concentrations employed for these experiments. Thus, effective permeability coefficients (P_{eff}) were calculated from the steady-state rate of appearance of the peptides and are summarized in Table II. Included in this table are previously determined permeability coefficients for transport of the peptides across rabbit intestinal mucosa (1,2).

For the Caco-2 cell studies, these permeability coefficients contain contributions from the permeability through the aqueous boundary layer (P_{aq}), across the monolayer ($P_{monolayer}$), and through the underlying filter (P_{filter}). Since these are resistances to diffusion in series, they are related by the following expression (9):

$$\frac{1}{P_{eff}} = \frac{1}{P_{aq}} + \frac{1}{P_{monolayer}} + \frac{1}{P_{filter}} \qquad (1)$$

which, on rearrangement, gives the permeability of the solute across the cell monolayer,

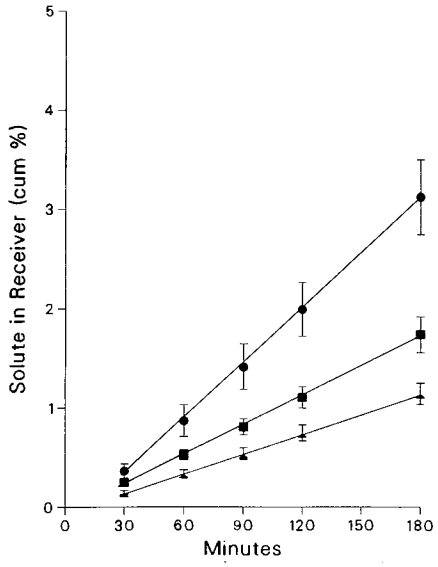

Fig. 2. Flux of the zwitterionic peptides I–III across confluent Caco-2 cell monolayers. Stock solutions of PheGly (●), Phe_2Gly (■), or Phe_3Gly (▲) were incubated in the Transwell system at 37°C. Each point represents the mean and standard deviation for at least three determinations.

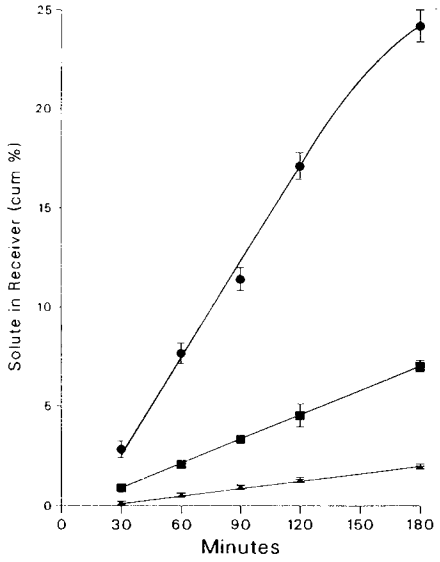

Fig. 3. Flux of the neutral peptides IV–VI across Caco-2 cell monolayers. Stock solutions of $AcPheNH_2$ (▲), $AcPhe_2NH_2$ (●), or $AcPhe_3NH_2$ (■) were incubated with Caco-2 cell monolayers at 37°C in the Transwell system. Each point represents the mean and standard deviation for at least three determinations.

$$P_{monolayer} = \frac{1}{\frac{1}{P_{eff}} - \frac{1}{P_{aq}} - \frac{1}{P_{filter}}} \qquad (2)$$

Thus, $P_{monolayer}$, the rate of transport across the Caco-2 cell monolayer, can be calculated if the aqueous diffusion layer permeability and the filter permeability are known. From a previous study, we determined P_{aq} to be 8×10^{-5} cm/sec for this Transwell model (6).

The permeability of the filter should be obtainable from measuring the rate of diffusion of the solute across an untreated, non Caco-2 cell containing Transwell insert. Because of technical problems, we were not able to perform this control experiment reproducibly. However, we do know that the filter permeability for the solutes is described by the following relationship:

$$P_{filter} = \frac{\epsilon D}{h} \qquad (3)$$

where ϵ is the porosity of the nucleopore filter (15%), h is the thickness of the filter (10 μm), and D is the diffusion coeffi-

Table II. Permeability Coefficients for Peptides I–VI

Peptide	P_{eff}[a] Caco-2	P_{eff}[a] Rabbit[b]	$P_{monolayer}$[a]
I	1.05 (0.28)	6.9 (1.9)	1.06 (0.3)
II	0.55 (0.11)	7.1 (0.9)	0.56 (0.10)
III	0.36 (0.07)	6.7 (3.2)	0.36 (0.07)
IV	7.99 (0.83)	14.0 (3.0)	8.85 (0.8)
V	2.20 (6.14)	5.0 (0.7)	2.26 (0.14)
VI	0.66 (0.03)	2.3 (0.4)	0.67 (0.03)

[a] cm/sec × 10^6. Values reported are the mean and standard deviation of at least three determinations.
[b] Data from Refs. 1 and 2.

cient of the solute through the filter pore. If the dimension of the pore is large with respect to the size of the molecule, then diffusion should be relatively uninfluenced by the pore walls and D should approach the value for free diffusion of the solute in solution.

For the solutes used in this study with molecular weights less than 550, we can estimate a reasonable molecular radius of 5–10 Å (10), while the pore diameter of the polycarbonate filter is 30,000 Å. Thus we expect these molecules to diffuse freely through the pore. Substituting a diffusion coefficient, $D = 8 \times 10^{-6}$ cm^2/sec, as a typical value for solutes of this size (11) into Eq. (3), we estimate P_{filter} to be about 1×10^{-3} cm/sec. Since this number is very large relative to P_{aq} and P_{eff}, it would be expected to have little influence on the transport rates of these solutes. Based on these considerations, P_{filter} was ignored in Eq. (2) and the values for $P_{monolayer}$ were determined. These results are also included in Table II.

Transport of Peptides I–VI Across Caco-2 Cell Monolayers as a Function of Lipophilicity. A plot of $P_{monolayer}$ for the zwitterionic and neutral peptides as a function of lipophilicity is shown in Fig. 4. As can be seen, increasing the peptide chain length in the charged series to three (II) and four (III) residues substantially increased the lipophilicity but resulted in a modest decrease in the observed permeability.

On the other hand, elimination of the charge to give the pseudo dipeptide IV improved transport markedly relative to the zwitterionic I. However, again increasing the phenylalanine content in this series, while improving lipophilicity, substantially reduced permeability with each amino acid added.

Transport of the Solutes as a Function of Hydrogen-Bond Number. In order to examine the premise that the permeability of these peptides could be correlated to the hydrogen-bonding potential, the number of hydrogen bonds (N) for each of the neutral peptides was estimated by use of the values in Table III as adapted from Stein (3). These results are summarized in Table IV. In order to increase the

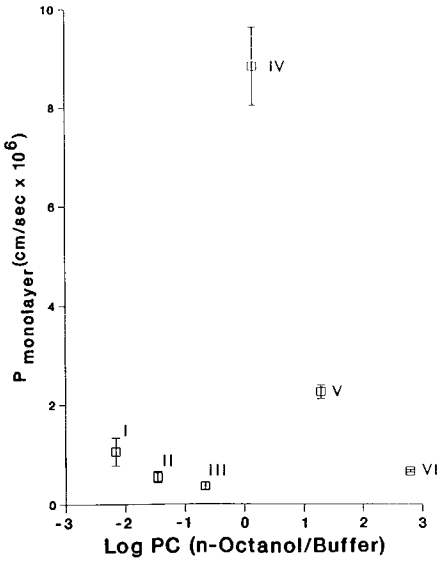

Fig. 4. The relationship between permeability coefficients and octanol–buffer partition coefficients for peptide solutes I–VI.

Table III. Assignment of Potential Hydrogen Bonds (N) to the Functionalities Present in the Peptides[a]

Function	Group in which present	N
–OH	Alcohol	2
$-NH_2$	Primary amine Primary amide	2
–N(R)H	Secondary amine Secondary amide	1
–CO–	Amide	1

[a] Adapted from Stein (3).

number of N values for the purpose of establishing a correlation, the transport of the primary, secondary, and tertiary amide solutes VII–IX was also examined. Similar to the results with the phenylalanyl oligomers, no evidence of metabolism was found in either the donor or the receiver compartments during the course of the transport studies for any of these solutes. The permeability coefficients were calculated and are shown in Table V.

With respect to the zwitterionic peptides I–III, a problem arises when trying to assign hydrogen-bonding values. For ionic species, as pointed out by Diamond and Wright, electrostatic interactions become dominant, making the hydrogen-bond concept less useful (12). Further, these hydrogen-bonding considerations apply only for a transport mechanism which involves diffusion of a molecule across the cell membrane. The $P_{monolayer}$ we have calculated contains this mechanism but also contains a contribution from paracellular diffusion, that is, diffusion between the cells rather than through the cell:

$$P_{monolayer} = P_{transcellular} + P_{paracellular} \quad (4)$$

In this case the contributions are additive since they are parallel pathways.

In contrast to diffusion across a cell membrane which involves a partitioning process, paracellular flux is via an aqueous pathway restricted by the presence of apical tight junctions between the cells (13). Since the solute does not leave the aqueous environment, desolvation is unnecessary and the principal determinant of the flux rate is the size of the molecule to the size of the aqueous "pore."

If the assumption is made that the flux of the zwitterionic peptides is restricted to the pore due to the charged nature of the solute, then the observed permeability can be used to approximate the dimensions of the paracellular junction in terms of an equivalent pore according to the relationship:

$$P = \frac{\epsilon DF(r/R)G_{el}}{h} \quad (5)$$

Table IV. Assignment of Hydrogen Bonds (N) to the Phenylalanine Peptides (IV–VI)

Peptide	N
IV	5
V	7
VI	9

Table V. Hydrogen-Bond Numbers (N) and Permeability Coefficients for the Model Solutes VII–IX

Solute	N	P_{eff}[a]	$P_{monolayer}$[a]
VII	3	54.3 (1.9)	170 (15)
VIII	2	58.0 (0.6)	211 (6)
IX	1	66.8 (1.3)	405 (38)

[a] cm/sec × 10^6. Values reported are the mean and standard deviation of at least three determinations.

where ϵ is the porosity of the membrane, D is the aqueous diffusion coefficient of the solute, h is the thickness of the membrane, G_{el} describes the charge density in the molecule, and $F(r/R)$ is the Renkin sieving factor, which relates the molecular radius of the solute (r) to the effective pore radius (14). By taking the ratio of the permeabilities between any two of the peptides, we get

$$\frac{P}{P'} = \frac{F(r/R)}{F(r'/R)} \tag{6}$$

where r and r' may be readily estimated as equivalent spheres by the Stokes–Einstein equation, and then R, the equivalent pore radius, becomes the only unknown. We have assumed that the molecular size effect on the diffusion coefficient and the distance of charge separation between the pairs of peptides are cancelled when the ratio is taken. The results of these calculations are shown in Table VI. As can be seen from this table, the permeability coefficients for peptides I–III suggest that these solutes are sieved through a pore that is approximately 8 Å in radius. It must be emphasized that this number is only a very crude estimate due to the limited data used in the determination but is useful as a first approximation.

Although the $P_{monolayer}$ calculated in this study contains contributions from $P_{paracellular}$ as well as $P_{transcellular}$, the relative contributions will depend upon the dimensions of the paracellular pore, the size of the solute, and the resistance of the solute to diffusion via the transcellular route. For very permeable substances, the paracellular route is expected to be relatively insignificant. On the other hand, for very poorly permeable solutes, the paracellular route may be the principal transport pathway. In theory, it should be possible to determine the para- and transcellular permeabilities for each of the solutes, but at the present time, an insufficient characterization of the molecular properties and pathways present in the system prevents us from doing so, but work in this regard is currently in progress and will be forthcoming in the future. Thus, with this qualification of $P_{monolayer}$ in mind,

Table VI. Estimation of Caco-2 Cell Monolayers' Effective Pore Size from the Permeability Results for the Zwitterionic Peptides (I–III)

Peptide	r(Å)	$F(r/R)$	R(Å)
I	4.52	0.0354	7.56
II	5.36	0.0228	8.66
III	5.99	0.0180	
Average			8.06

the permeabilities from Tables I and V and the N values for the solutes were used to obtain the plot shown in Fig. 5.

DISCUSSION

The results shown here for the transport of peptides I to VI across Caco-2 cells are qualitatively identical to our earlier results with the same peptides in an *in vitro* rabbit intestinal model. In both cases, the permeability is low in the charged series, and while increasing the phenylalanine content increased the octanol distribution coefficient, the permeability is decreased. Further, a significant increase in flux is found by elimination of the charge to give the dipeptide IV, but again, increasing the phenylalanine content reduces transport, despite a significant increase in lipophilicity.

These results are in marked contrast to what was found for the relationship of permeability with lipophilicity in the Caco-2 cell model with a simpler series of model solutes (6). There, a sigmoidal relationship was established, with permeability approaching a maximum value as the log octanol–water partition coefficient was increased to about 2. No such correlation was found here. Indeed, with the neutral peptides IV–VI, almost the exact opposite dependence is seen; that is, increasing the log PC results in lowered permeabilities. The last member in the series, $AcPhe_3NH_2$, has a log PC of 2.8, which should put it within the aqueous boundary layer control limit for absorption (6). Thus, it seems clear that some other factor is controlling the permeability of the peptides in this system.

As we discussed in our earlier rabbit work, the progression through the series I–III and IV–VI involves the addition of two amino acids. While this increase should be accompanied by a favorable increase in lipophilicity due to the large hydrocarbon side chain of phenylalanine (15), we are also introducing a very polar amide bond into the chain with each residue. Such polar functionalities are capable of forming strong interactions with hydrogen-bonding solvents (16).

For these solutes, then, we can consider the partitioning

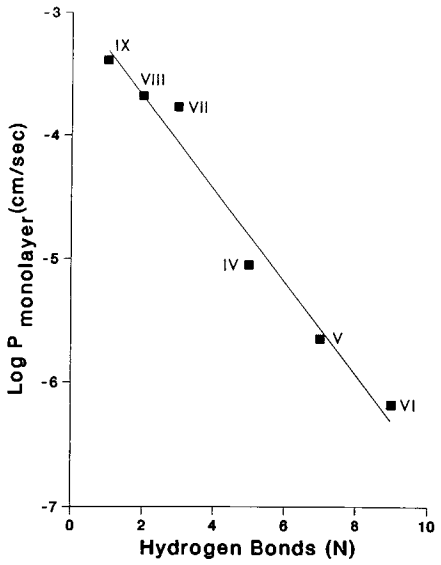

Fig. 5. Relationship of the permeability coefficients for solutes IV–IX across Caco-2 cell monolayers and number of potential hydrogen-bonding sites in the solute.

process into octanol as consisting of two components. The first is a hydrophobic effect which arises from the unfavorable entropy accompanying the dissolution of nonpolar residues in water. In fact, it has been shown that the ΔG for transfer of the phenylalanine side chain from water into hydrocarbon is -3.24 kcal/mol (17). This provides a strong driving force for the movement of these peptides from water into the octanol phase.

The second component arises from the presence of the strong hydrogen bonds these solutes can form with water. Energy must be expended to break these bonds in order for the solute to reach the transition state for transfer from one phase to the other (16). Since octanol is a hydrogen-bonding solvent, these broken solute–water bonds can be satisfied by the octanol. Thus the overall energy required for the desolvation step in the transfer process will be small. In this case, the partition coefficient will be more representative of the hydrophobic effect and little influenced by hydrogen-bonding considerations. This is why we see such large increases in octanol partitioning with each phenylalanine residue added to the chain.

Similarly, diffusion across a cell membrane involves a partitioning process, that is, movement of the solute from the aqueous medium into the membrane interior. If, as has been suggested, the membrane is more hydrocarbon like, with little or no hydrogen-bonding potential (18), then the favorable hydrophobic component favoring transfer will be opposed by the desolvation energy. Since it has been estimated that the energy cost of transferring an amide bond from water into hexane is 6.1 kcal/mol (19), this step can represent a significant barrier to the diffusion of such molecules. Indeed, our results suggest that this is the dominant force controlling the transport of these peptides across both rabbit and Caco-2 cell membranes.

The importance of hydrogen bonding in predicting solute transport across cells is analogous to what Stein showed for the uptake of small molecules into the giant algae *Chara* and similar studies with other cells, including mammalian erythrocytes (3). However, whereas Stein included in his treatment many different hydrogen-bonding functionalities, we have chosen to restrict our studies to amides and related groups likely to be encountered in amino acids, since our primary interest is in peptides. Nevertheless, it seems clear from the results shown in Fig. 5 that a strong argument for the negative impact of hydrogen-bonding groups on peptide transport can be made.

In summary, we find that the transport of the model peptides I–VI across Caco-2 cell monolayers is similar to results obtained from rabbit intestinal mucosa. Again, as with the rabbit, there is no obvious correlation between the transport of these peptides and the octanol–water partition coefficient of the peptide. There is, however, a strong correlation between the permeability of the peptides and the number of hydrogen bonds the solute can make with water, which must be broken in order for the solute to transfer into the cell membrane interior. These results should offer a simple method for ranking the absorption potential of newly synthesized peptides or guiding in the design of compounds with good absorption potential. These results further suggest that chemical modification to improve absorption of existing structure, perhaps via the prodrug approach, should focus on modifications which decrease the total hydrogen-bonding potential of the molecule.

Finally, we recognize that treating all potential hydrogen bonds as energetically equivalent, as is implicit in Table III, is a naive approximation. However, as the results here show, it can be useful. Future work will present experimental methods to measure the desolvation energy of a peptide directly, similar to the partition coefficient difference method used to guide the synthesis of histamine antagonists with improved blood–brain barrier permeability (20). This should prove useful for the study of inductive and steric factors, among others, which will influence hydrogen-bond strength. Such effects will not be obvious by simple inspection of the peptide primary sequence.

ACKNOWLEDGMENTS

We would like to thank R. Blake Hill for excellent technical assistance during the course of this work. We also thank Brenda Mussulman for preparation of the manuscript.

REFERENCES

1. P. S. Burton, R. B. Hill, and R. A. Conradi. Metabolism and transport of peptides across the intestinal mucosa. *Proc. Int. Symp. Control. Rel. Bioact. Mater.* 14:6–7 (1987).
2. N. F. H. Ho, J. S. Day, C. L. Barsuhn, P. S. Burton, and T. J. Raub. Biophysical model approaches to mechanistic transepithelial studies of peptides. *J. Control. Release* 11:3–24 (1990).
3. W. D. Stein. The molecular basis of diffusion across cell membranes. In *The Movement of Molecules Across Cell Membranes,* Academic Press, New York, 1967, pp. 65–125.
4. I. J. Hidalgo, T. J. Raub, and R. T. Borchardt. Characterization of the human colon carcinoma cell line (Caco-2) as a model system for intestinal permeability. *Gastroenterology* 96:736–749 (1989).
5. G. Wilson, I. F. Hassan, C. J. Dix, I. Williamson, R. Shah, and M. Mackay. Transport and permeability properties of human Caco-2 cells: An in vitro model of the intestinal epithelial cell barrier. *J. Control. Release* 11:25–40 (1990).
6. A. R. Hilgers, R. A. Conradi, and P. S. Burton. Caco-2 cell monolayers as a model for drug transport across the intestinal mucosa. *Pharm. Res.* 7:902–910 (1990).
7. A. I. Vogel. *A Textbook of Practical Organic Chemistry,* Longmans, Green and Co., London, 1959.
8. A. H. Lewin, M. Frucht, K. V. J. Chen, E. Benedetti, and B. D. DiBlasio. Restricted rotation in amides VI. Configurations and conformations of unsymmetrical tertiary benzamides. *Tetrahedron* 31:207–215 (1975).
9. N. F. H. Ho, J. Y. Park, P. F. Ni, and W. I. Higuchi. Advancing quantitative and mechanistic approaches in interfacing gastrointestinal drug absorption studies in animals and humans. In W. Crouthamel and A. C. Sugars (eds.), *Animal Models for Oral Drug Delivery in Man,* Am. Pharm. Assoc., Washington, DC, 1983, pp. 27–106).
10. E. M. Renkin. Filtration, diffusion and molecular sieving through porous cellulose membranes. *J. Gen. Physiol.* 38:225–238 (1954).
11. H. Westergaard and J. M. Dietschy. Delineation of the dimensions and permeability characteristics of the two major diffusion barriers to passive mucosal uptake in the rabbit intestine. *J. Clin. Invest.* 54:718–732 (1974).
12. J. M. Diamond and E. M. Wright. Molecular forces governing non-electrolyte permeation through cell membranes. *Proc. Roy. Soc. B* 172:173–316 (1969).
13. J. L. Madara. Loosening tight junctions. *J. Clin. Invest.* 83:1089–1094 (1989).
14. N. Lakshminarayanaiah. In *Equations of Membrane Biophysics,* Academic Press, New York, 1984.

15. G. O. Rose, A. R. Geselowitz, G. J. Lesser, R. H. Lee, and M. A. Zehfus. Hydrophobicity of amino acid residues in globular proteins. *Science* **229**:834–838 (1985).
16. I. M. Klotz and S. B. Farnham. Stability of an amide-hydrogen bond in an apolar environment. *Biochemistry* 7:3879–3882 (1968).
17. M. A. Roseman. Hydrophilicity of polar amino acid side-chains is markedly reduced by flanking peptide bonds. *J. Mol. Biol.* **200**:513–522 (1988).
18. J. M. Diamond and Y. Katz. Interpretation of nonelectrolyte partition coefficients between dimyristoyllecithin and water. *J. Membr. Biol.* **17**:121–154 (1974).
19. M. A. Roseman. Hydrophilicity of the peptide CO ·· NH hydrogen-bonded group. *J. Mol. Biol.* **201**:621–623 (1988).
20. R. C. Young, R. C. Mitchell, T. H. Brown, C. R. Ganellin, R. Griffiths, M. Jones, K. K. Rana, D. Saunders, I. R. Smith, N. E. Sore, and T. J. Wilks. Development of a new physicochemical model for brain penetration and its application to the design of centrally acting H_2 receptor histamine antagonists. *J. Med. Chem.* **31**:656–671 (1988).